Original article

Ferula ferulaeoides ethyl acetate extract induces apoptosis in esophageal cancer cells via mitochondrial and PI3K/Akt/Bad pathways

Yerlan Bahetjan [a], Wenqi Liu [a], Muguli Muhaxi [b], Ni Zheng [a], Fatemeh Sefidkon [c], Kejian Pang [b], Guangwen Shu [a,*], Xinzhou Yang [a,*]

[a] School of Pharmaceutical Sciences, South-Central Minzu University, Wuhan 430074, China
[b] College of Biological Sciences and Technology, Yili Normal University, 835000, Yili, China
[c] Research Division of Medicinal Plants, Research Institute of Forests and Rangelands, Agricultural Research Education and Extension Organization (AREEO), P.O. Box 13185-116, Tehran, Iran

ARTICLE INFO

ABSTRACT

Background: Ferula ferulaeoides (Steud.) Korovin is a traditional ethnopharmacological plant used for lump elimination and as a spice, especially in places like India. It has also been employed in the livestock and food industries. This investigation aimed to explore the anti-tumor mechanisms of ethyl acetate extract fractions of dried roots of *Ferula ferulaeoides* (FF-EtOAc) on esophageal cancer (EC) cells. Furthermore, it was hypothesized that FF-EtOAc could inhibit EC cells growths by inducing apoptosis.
Results: In a time- and dose-dependent manner, FF-EtOAc considerably reduced the number of migrating EC cells. And FF-EtOAc also inhibited the growth of EC cells *in vivo*, and it is less toxic to nude mice. In terms of the FF-EtOAc anticancer mechanism, the findings revealed that FF-EtOAc inhibited EC cells growth by activating mitochondrial signaling pathways and PI3K/Akt/Bad signaling pathways.
Conclusions: Through both *in vitro* and *in vivo* experiments, FF-EtOAc significantly exhibited anti-esophageal cancer activity. The anti-EC activity of FF-EtOAc may be due to the activation of the mitochondrial apoptotic and PI3K/Akt/Bad signaling pathways.
© 2023 The Author(s). Published by Elsevier B.V. on behalf of King Saud University. This is an open access article under the CC BY-NC-ND license (http://creativecommons.org/licenses/by-nc-nd/4.0/).

1. Introduction

Cancer, which ranks as the second leading cause of death globally (Ahmed et al., 2022), is a significant burden on the medical

Production and hosting by Elsevier

profession all over the world. According to the World Health Organization, "One in every five men and one in every six women in the world develop cancer during their lifetime" (Bray et al., 2018). In 2020, China accounted for 25% of all cancer deaths worldwide (Sung et al., 2021). Among them, Esophageal cancer (EC) has the sixth-highest incidence and fourth-highest fatality rates in China (He et al., 2021). One of the deadly gastrointestinal malignancies is esophageal cancer (Watanabe et al., 2020). The histological subtypes of esophageal cancer are classified into adenocarcinoma and squamous cell carcinoma, with squamous cell carcinoma being the most prevalent. And the most prevalent regions for squamous cell carcinoma are China (47%) and Central Asia (19%) (Homs et al., 2009, Li et al., 2018). Treatment options for esophageal cancer include surgery, chemotherapy, and radiation therapy (Kato and Nakajima 2013). Despite surgical techniques with great advancements, esophageal cancer has a poor prognosis. Chemotherapy and radiotherapy are also used only as adjuvant methods, and they are harmful to the human body. Although Western medicine has played a primary role in cancer treatment and has made significant breakthroughs in curing cancer in recent years, its prognosis remains unsatisfactory (Howell and Shalet 1998, DeHaven 2014, Kakeji et al., 2021). Because of low toxicity and easy availability,

etc, natural products gained popularity in anti-cancer drug research(Atanasov et al., 2021).

The genus *Ferula* L. is an angiosperm Umbelliferae plant, there are more than 180 species of *Ferula* L. in the world (Salehi et al., 2019), and these plants are mainly distributed in Central Asia, the Middle East, Siberia, South Asia, and Northwest China (Znati et al., 2014). Due to natural origin and low toxicity, *Ferula* L. is used extensively in people's daily life. In traditional use, it is added to food as a spice and it was also used in pickles (Mahendra and Bisht 2012). And in modern life, Ferula was used in grazier, food and medicine (Sonigra and Meena 2020), such as antiprotozoal (Bashir et al., 2014), antihelmintic (Tavassoli et al., 2018), antioxidant (Rahali et al., 2018), antimicrobial (Utegenova et al., 2018), antidiabetic (Yarizade et al., 2017), insecticidal (Liu et al., 2020), and anticancer activities (Asemani et al., 2018).

Ferula ferulaeoides, a notable species of the genus *Ferula* L. and a unique plant resource in the Xinjiang region of China, and it is mainly distributed in dunes, sandy land, and other places in Xinjiang. In Xinjiang, *F. ferulaeoides* leaves have been used as vegetables for cooking, and its roots and resin are used for medicinal purposes. *F. ferulaeoides,* in addition to eliminating lumps, and is also used to treat cold pains in the heart and abdomen, malaria, and dysentery (Chinese Pharmacopoeia Commission 2020). The anti-cancer effect of *F. ferulaeoides* has been reported, such as malignant peripheral nerve sheath tumor, breast cancer, and skin cancer (Sattar and Iranshahi 2017, Li et al., 2018, Yao et al., 2020), but antiesophageal cancer activity and action mechanisms are less well studied. Our study showed that FF-EtOAc could inhibit the activity of EC cells *in vivo* and *in vitro*, and the potential mechanism action of FF-EtOAc on esophageal cancer was initially explored. Further cytotoxicity experimentation showed that the FF-EtOAc has low cytotoxicity.

2. Materials and methods

2.1. Plant material

The roots of *Ferula ferulaeoides* (Steud.) Korovin were collected in Shihezi City, Xinjiang Uygur Autonomous Region, China, in May 2019, and identified by Professor Kejian Pang (Shihezi University, Shihezi, China). In the School of Pharmaceutical Sciences at South-Central Minzu University in Wuhan, China, a voucher specimen (No. SC0426) was deposited.

2.2. Preparation and chemical interpretation of FF-EtOAc

Mechanically crushed *F. ferulaeoides* roots had been air-dried, and 90 g of the powder was used for extracting by speed extraction at 80℃, 10 MPa with petroleum ether, ethyl acetate, and methanol (each solvent, 4 cycles; each cycle 15 min) to yield petroleum ether extract (4.03 g), ethyl acetate extract (FF-EtOAc, 10.27 g) and methanol extract (6.11 g), and the extraction rates were 4.47%, 11.4%, and 6.78%.

The chemical profile of FF-EtOAc was conducted by UPLC-Q-TOF-MS, and it was employed by using an ultra-high performance liquid chromatography (UPLC) system (Waters Corp, Manchester, England) consisting of a binary pump, a degasser, an autosampler, and a column compartment with a high throughput G2Si High-definition mass spectrometer (Waters Q-TOF SYNAPTTM, Waters Corp, Manchester, England), and equipped with an electrospray (ESI) interface. A Waters ACQUITY UPLC HSS T3 column (100 mm × 2.1 mm, 1.8 μm) was used for the chemical profiling of FF-EtOAc. The 0.1% aqueous formic acid (A) and acetonitrile (B) made up the mobile phase. This system was used for chromatographic separation at 25 °C. Gradient elution with a flow rate of 0.4 mL/min was performed as follows: 2% − 95% B at 0−−25 min. Leucine enkephalin was employed as the precise mass calibration solution for the MS analysis, which was conducted using an electrospray ionization (ESI) source in both positive and negative ion modes. 350 °C was the temperature of the desolvation gas. Cone and desolvation gas flow rates were established at 50 L/h and 600 L/h, respectively. In the positive and negative ion modes, the capillary, cone, and extraction cone voltages were set to 3.0 and 2.5 V, respectively. With a low collision energy of 6 V and a high collision energy of 20–80 V, MSE was used for MS/MS analysis. The scan area was set at *m/z* 50–1200.

2.3. Chemicals and reagents

The MTT chemicals were from neoFroxx (Einhausen, Germany), and the Annexin V-FITC/PI Double-stained Apoptosis Detection Kit came from BestBio (Shanghai, China). The Hoechst 33258 reagents, BCA protein quantification kit, SDS–PAGE sample loading buffer, and RIPA lysis solution were purchased from Beyotime Biotechnology (Nantong City, Jiangsu Province, China). We purchased the eECL Western blot Kit from Bioprimacy (Wuhan China). Dulbecco's modified eagle medium (DMEM) and Roswell Park Memorial Institute (RPMI) 1640 were purchased from Hyclone (Logan, UT, USA). Fetal bovine serum (FBS) from Newzerum (Christchurch New Zealand) and antibiotics (100 U/mL penicillin and 100 μg/mL streptomycin) were obtained from Hyclone (Logan, UT, USA). Antibodies of MMP-9, Bcl-2, Caspase-3, PARP, Akt, p-Akt (Ser473), Bad, p-Bad (Ser136), p-GSK-3α/β (Ser 21/9), GSK-3α/β and PTEN were obtained from Cell Signaling Technology (Danvers, MA, USA). Caspase-9 and Bax were purchased from ABclonal Biotech (Wuhan, Hubei, China). β-actin was obtained from Bioprimacy (Wuhan China). We purchased the matching secondary antibody from ABclonal Biotech (Wuhan, Hubei, China).

2.4. Cell culture

The human embryonic kidney (HEK) cell lines HEK293 and esophageal cancer (EC) cells (Eca-109 and KYSE150) were purchased from the American Type Culture Collection (Manassas, USA). Eca-109 cells, KYSE-150 cells, and HEK293 cells were grown in a medium containing 90% DMEM or RPMI-1640, 10% FBS, and 1% antibiotics (100 U/mL penicillin and 100 g/mL streptomycin), DMEM is used for Eca-109 cells and HEK-293 cells and RPMI-1640 is used for KESE-150 cells. These cells were cultured in a cell culture incubator (Heal Force, Shanghai, China). The culture conditions were set at 5% CO_2, 37 °C.

2.5. Cell viability test

The noxiousness of FF-EtOAc toward the Eca-109, KYSE150, and HEK293 cell lines was assessed using the MTT test. Eca-109, KYSE150, and HEK293 cells (1×10^5 cells/well) were planted in 96-well plates and cultivated until 90% confluence was reached. Then, 0, 10, 20, 30, 40, and 50 μg/mL FF-EtOAc was applied to Eca-109 and KYSE150 for 6, 12, or 24 h, and HEK293 cells for 12 h. After treating over and discarding the FF-EtOAc, MTT (5 mg/mL) was administered to each well for 30 min in a culture incubator with 37 °C and 5% CO_2. Then, aspirate the MTT solution and add 150 mL of DMSO to each well before using a microplate reader to measure the optical density (OD) value at 570 nm. (Thermo Scientific, CA, USA). Calculating the inhibition rate uses the following formula: inhibition rate (%) = [1 − (OD $_{sample}$ − OD $_{blank}$) / (OD $_{control}$ − OD $_{blank}$)] × 100 (Chen et al., 2019). The concentration of FF-EtOAc at which the cell inhibition rate was 50% as determined by MTT assays and estimated by the GraphPad Prism

8.0 Software (GraphPad Prism Software, Inc.) is known as the IC$_{50}$ value.

2.6. Histological morphology and Hoechst 33258 staining of cells

EC cells were sowed in 6-well plates (2 × 10^5 cells/well) and cultivated until 90% confluence was achieved. The EC cells were treated with 0, 10, 20, and 30 µg/mL FF-EtOAc within 12 h. Then using an inverted phase contrast microscope, the cellular morphological alterations were captured at a 20 × magnification (Nikon, ECLIPSE-Ti, Japan). Following treatment, the cells were treated with Hoechst 33258 solution (5 µg /mL) for 30 min in the dark before being fixed for 15 min with a fixing solution (methanol: acetic acid = 3: 1). Then, a fluorescent inverted microscope (Nikon, ECLIPSE-Ti, Japan) was used to observe the cell morphology before a 40 × magnification photograph was taken.

2.7. Cell migration assay

EC cells in the logarithmic phase were seeded on a 6-well plate (1 × 10^5 /mL /well) for the cell migration experiment. EC cells were treated with 0, 5, 7.5, and 10 µg/mL FF-EtOAc for 12 and 24 h. Using a 200 µL pipette tip, the center of each well was scratched. Scratch images were then captured after 0, 12, and 24 h at a magnification of 20 ×. ImageJ was used to measure and record the scratch width.

For the Transwell migration assay, EC cells were inoculated in Transwell upper compartment (Corning, NY, USA) for 12 h, lower compartment with DEME, or 1640 without FBS. The FF-EtOAc solution was added to the upper compartment and treated with 0, 5, 7.5, and 10 µg/mL FF-EtOAc for 12 h. After drug advertising has ended, absorb and clean the upper compartment and lower compartment. Next, fixed with anhydrous ethanol for 10–20 min and cleaned three times with ultrapure water. The fluorescence inverted microscope was for observing the amount of cell movement and crystalline violet staining. In three randomly selected fields, the number of cells moving through the membrane was counted. The experimental results were analyzed by ImageJ.

2.8. Annexin V-FITC/PI double staining assay and measurement of apoptosis

EC cells were sowed into 6-well plates (2 × 10^5 cells/well), and cultivated until 70% − 80% confluence was achieved. Within 12 h, the EC cells were treated with 0 and 30 µg/mL FF-EtOAc. The EC cells were digested with trypsin without ethylenediaminetetraacetic acid (EDTA) (Hyclone, Logan, UT, USA) and centrifuge at approximately 300–500 g force, 2–8 °C, 5 min, and the suspended cells were collected. Next, the EC cells were washed four times with cold PBS (Hyclone, Logan, UT, USA) and centrifuged. Then, 400 µL Annexin V Binding Buffer (1 ×) was added to suspend the cells. Add 5 µL of Annexin V-FITC (EGFP/Alexa Fluor488) staining solution to the cell suspension, blend and incubate for 15 min at 2–8 ℃ under light-proof conditions. Add 5–10 µL of PI staining solution and gently mix and incubate for 2–5 min at 2–8 °C under light-proof conditions. After staining and qualitative fluorescence microscopy examination, using flow cytometry, the percentage of apoptotic cells was determined. The percentage of apoptotic cells was examined using FlowJo10 software.

2.9. Protein extraction and Western blot analysis

EC cells were seeded into 6-well plates (2 × 10^5 cells/well) and cultivated until 70% − 80% confluence was achieved. Then incubated with 0, 10, 20, and 30 µg/mL FF-EtOAc for 24 h, the EC cells were collected by centrifugation and lysed in radioimmunoprecip-

itation assay (RIPA) lysis buffer (Beyotime, Shanghai, China), phosphatase inhibitor cocktail A (Beyotime, Shanghai, China) and phenylmethanesulfonylfluoride or phenylmethylsulfonyl fluoride (PMSF) (Boisharp, Hefei, China) to extract the proteins. The protein concentration in the supernatant was measured using the bicinchoninic acid (BCA) kit (Beyotime, Shanghai, China). Then, the protein was stored at −80 °C until required. The same produced for protein extraction from rat tumor tissue was used. Similar sums of the protein were isolated by 10 % or 12.5 % SDS-PAGE gel electrophoresis (Epizyme Biomedical Technology, Shanghai, China) at room temperature and transferred to polyvinylidene difluoride (PVDF) membranes (Bio-Rad, CA, USA) on the ice. The membranes were jammed by 5% Bovine serum albumin (BSA) tris-buffered saline with tween 20 (0.5%) for 2 h. Subsequently, the membranes were incubated with the secondary antibody (1: 10000) at 37 °C for 2 h after being combined with the primary antibody (1: 1000) at 4 °C for overnight. The HRP ECL system (Bio-Rad, CA, USA) is a tool used to visualize protein bands and it is used for our protein bands. The Grayscale values are used for data analysis by Image lab software.

2.10. EC-bearing nude mouse and in vivo treatment

The four weeks old of athymic nude mice were bought from Beijing HFK Biological Science Co., Ltd. (SCXK 2019–0008). The proper institutional, national, and/or international standards for the handling and usage of animals were adhered to. The Experimental Animal Care and Use Committee of South-Central Minzu University's ethical guidelines were followed at all times when using animals in research. After all nude mice were acclimatized for one week. By subcutaneously injecting Eca-109 cells into the mouse's right side of the back, the model of an Eca-109-bearing nude mouse was produced (He et al., 2013, Huang et al., 2020). When the nude mouse's tumor volume achieved 100 mm^3, they were stochastically divided into 3 groups and treated with 0, 60, and 120 mg/ kg FF-EtOAc every other day for 21 days. The nude mouse's tumor volume was measured by a vernier caliper every other day. Tumor volume (V) was calculated as described below: V = 0.5 × width^2 × length. After 21 days of FF-EtOAc treatment, nude mice were dissected and collected for further analysis of transplanted tumors along with the liver, kidney, and spleen. The Experimental Animal Care and Use Committee of South-Central Minzu University's ethical guidelines were followed in animal experiments and approved (Approval Number: S08921080A).

2.11. TdT-mediated dUTP nick-end labeling (TUNEL assay)

Each specimen of the xenograft mice tissues was cut into slices, fixed, and then embedded in paraffin for TUNEL staining. Following TUNEL analysis, 200 × magnification photos were taken of each tumor fraction.

2.12. Immunohistochemistry (IHC) assay

Each section of the xenograft mice tissues was chosen for immunohistochemistry, and the primary antibody was incubated with it before the corresponding peroxidase-conjugated horseradish secondary antibody was incubated with it and coating for observation. The tumor samples were captured on camera with 200 × magnification.

2.13. Hematoxylin-eosin (HE) staining

Each section of xenograft of nude mice samples was stained hematoxylin and eosin. The tumor samples were captured on camera with 200 × magnification.

2.14. Statistical analysis

Three independent experiments are used to calculate the mean and SD of each set of data. Statistics were analyzed using GraphPad Prism 8.0 Software. ANOVA was used to analyze statistical differences between the FF-EtOAc treated groups, and P values < 0.05 were considered significant (*P < 0.05, **P < 0.01 or ***P < 0.001).

3. Results

3.1. Chemical composition analysis of FF-EtOAc

The roots of *F. ferulaeoides* were dried and speed-extracted to produce FF-EtOAc. By searching databases such as China National Knowledge Infrastructure, PubMed, PubChem, and Reaxys, we obtained the complete compound information for *F. ferulaeoides*. And a self-building database of chemical compounds was established by UNIFI software, including relative molecular mass, molecular formula, CAS number, and mol file of structural formula for each chemical composition. Among them, a total of 42 compounds were listed. High-resolution mass spectrometry data of the main chemical constituents of FF-EtOAc were rapidly acquired by the UPLC-Q-TOF/MS method. The base peak intensity (BPI) chromatograms of FF-EtOAc in the negative and positive ion modes and the basic peak intensity (BPI) chromatograms of FF-EtOAc from in

the ultraviolet mode were shown in Fig. 1. We utilized the UNIFI information management platform for swift matching of its mass spectrometry data. Upon closer manual examination, 10 principal chemical constituents were identified in FF-EtOAc, predominantly furanocoumarins. Detailed insights into these constituents can be found in Fig. 1, Fig. 2, and Table 1.

3.2. Effect of FF-EtOAc on the proliferation and morphology of EC cells

The anti-proliferative effect of FF-EtOAc on EC cells was evaluated by MTT assay, and the IC_{50} values and cell survival rates of FF-EtOAc were obtained (Fig. 3A and B). FF-EtOAc had lower toxicity to HEK293 cells than the other two types of EC cells (Fig. 3C). Furthermore, observation of cell morphology through an inverted microscope showed that FF-EtOAc induced cellular shrinkage, floating, deformation, and detachment from the cell matrix (Fig. 3D). The results showed that FF-EtOAc markedly suppressed EC cells viability and proliferation *in vitro*.

3.3. Effect of FF-EtOAc on the migration of EC cells

Cell migration is the basis for establishing and maintaining the normal organization of multicellular organisms, and restraining the migration of cancer cells is one way to reduce the spread of highly malignant cancer cells (Trepat et al., 2012). The effects of
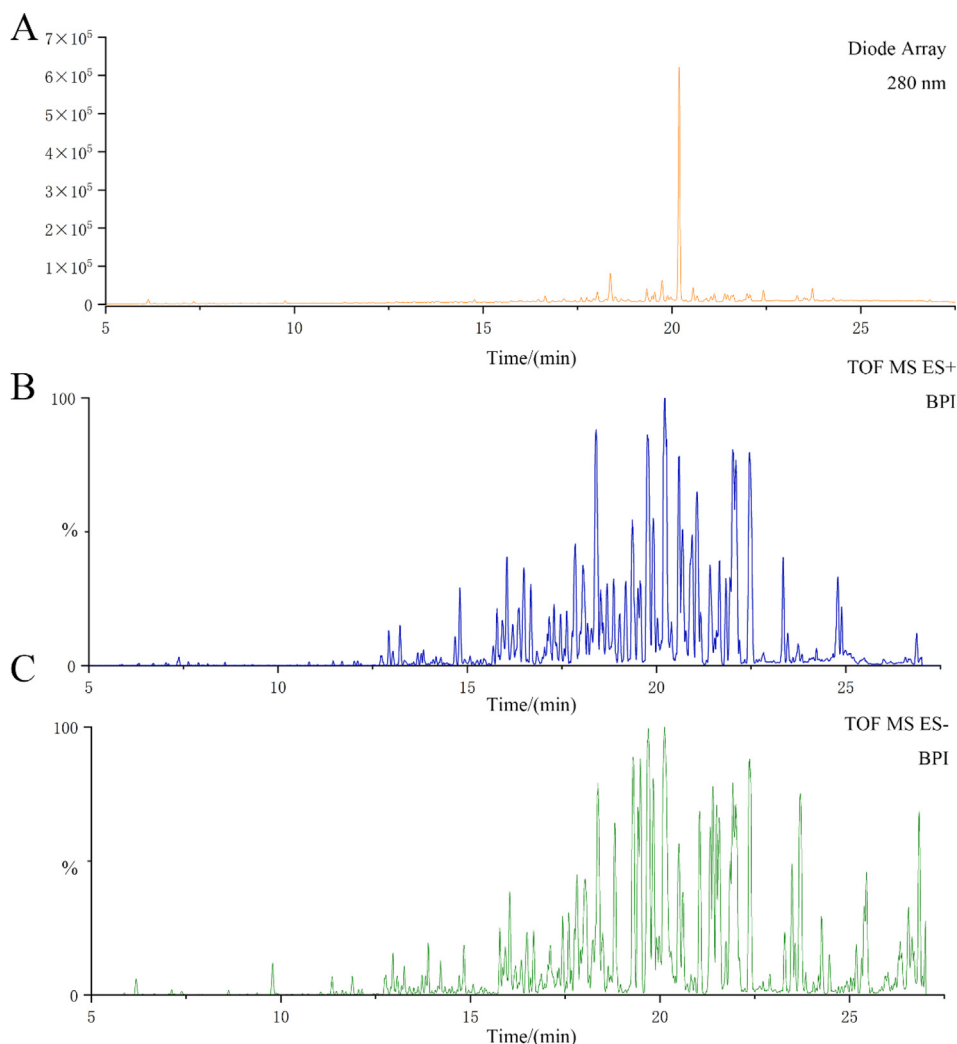
Fig. 1. UPLC-Q-TOF/MS analysis of FF-EtOAc. (A) The basic peak intensity (BPI) chromatogram of FF-EtOAc from UPLC-Q-TOF/MS analysis in the ultraviolet mode at 280 nm. (B) The ESIMS chromatogram of FF-EtOAc in the positive ion mode. (C) The ESIMS chromatogram of FF-EtOAc in the negative ion mode.
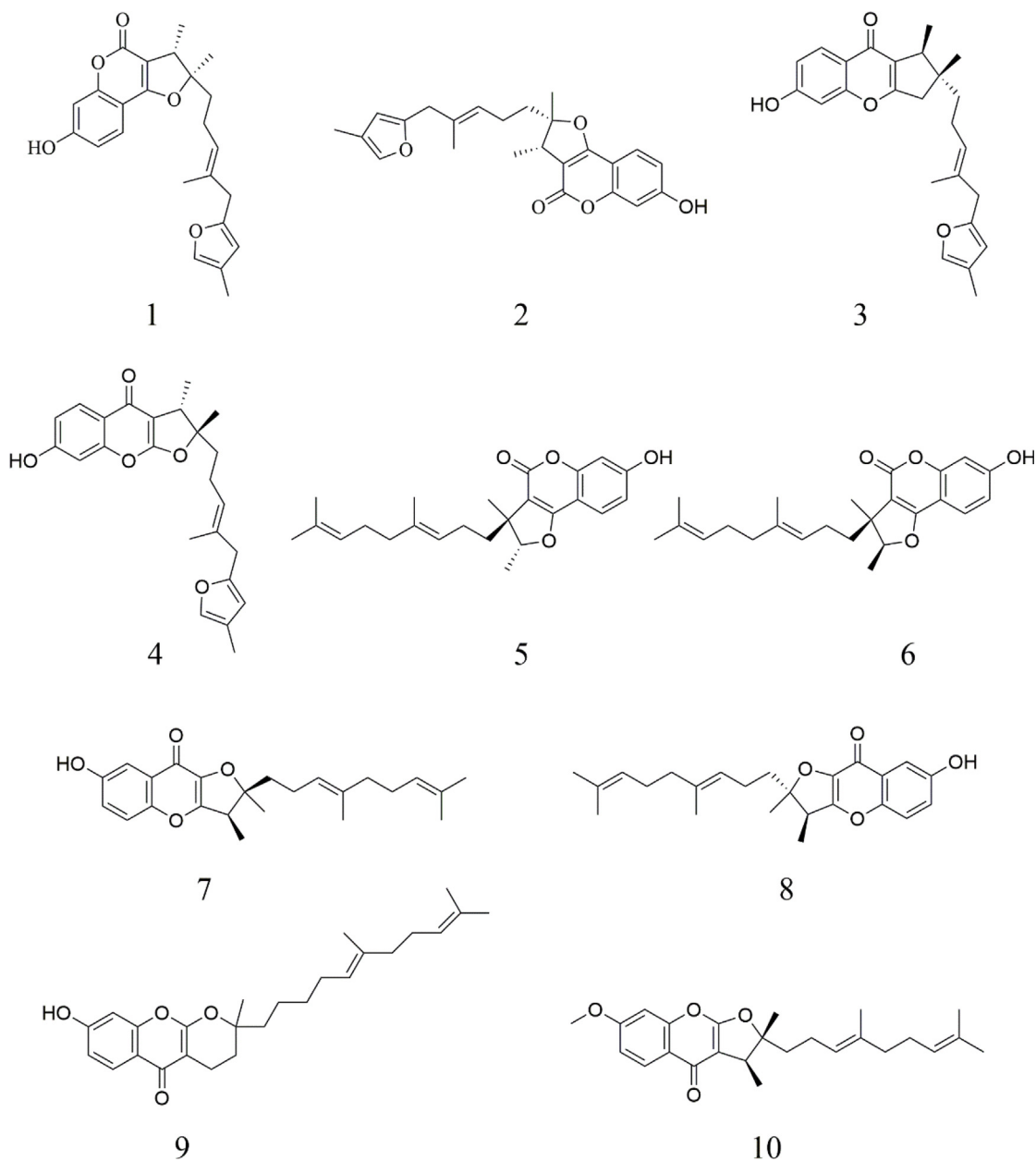
Fig. 2. Structural diagram of the chemical components in FF-EtOAc.

FF-EtOAc on EC cell migration were investigated using both scratch tests and Transwell assays. The expression of Matrix Metalloproteinases is associated with matrix remodeling, particularly cancer invasion, and angiogenesis (Shay et al., 2015). This will be investigated as a mechanism of action, whereby we examined the expression of relevant proteins. The FF-EtOAc suppressed the migration and quantity of EC cells in a dose-dependent relationship as compared to the blank group, according to the comparison of the aforementioned experimental data, and monitoring of MMP-9 expression revealed that FF-EtOAc suppressed MMP-9 expression (Fig. 4A-4D). Meanwhile, Transwell experiments demonstrate the same results (Fig. 4E).

3.4. Effects of FF-EtOAc on apoptosis of EC cells

The apoptotic effect of FF-EtOAc on EC cells cultivated *in vitro* was evaluated using Annexin V-FITC/PI, Hoechst 33258, and flow cytometry. After treated with FF-EtOAc for 12 h, EC cells have chromatin compression in their nuclei and the presence of apoptotic body, which are characteristic manifestations of apoptosis. And the number of cells with these characteristics increases with increasing dose (Fig. 5A). Results from flow cytometry and Annexin V-FITC/PI analysis demonstrated that FF-EtOAc caused EC cells to apoptosis in a dose-dependent way (Fig. 5B and 5C).

3.5. Mitochondrial apoptosis and PI3K/Akt/Bad pathways are the main pathways of FF-EtOAc induction of apoptosis in vitro

F. ferulaeoides has been reported to inhibit cancer cell proliferation and promote apoptosis through the mitochondrial pathway and downregulate the expression of phosphorylated Akt (Kim et al., 2011, Zhang et al., 2015). In addition, downregulation of phosphorylated Akt expression phosphorylates downstream GSK-3 α/β and Bcl-2-associated death promoter (Bad) proteins, thereby

Table 1
Identification and Analysis of Chemical Constituents in FF-EtAc by UPLC-Q-TOF/MS.

No.	Molecular iron(m/z)	Exact mass	Molecular formula	Ion type	Compound	Reference
1	395.1852	395.1853	$C_{24}H_{27}O_5$	[M + H]$^+$	2,3-dihydro-7-hydroxy-2S*,3R*-dimethyl-2-[4-methyl-5-(4-methyl-2-furyl)-3(E)-pentenyl]-furo[3,2-c]coumarin	(Isaka et al., 2001)
2	395.1887	395.1853	$C_{24}H_{27}O_5$	[M + H]$^+$	2,3-dihydro-7-hydroxy-2R*,3R*-dimethyl-2-[4-methyl-5-(4-methyl-2-furyl)-3(E)-	(Isaka et al., 2001)
3	395.1857	395.1853	$C_{24}H_{27}O_5$	[M + H]$^+$	pentenyl]-furo[3,2-c]coumarin2,3-Dihydro-7-hydroxy-2S*,3R*-dimethyl-2-[4-methyl-5-(4-methyl-2- furyl)-3(E),7-pentenyl]-furo[2,3-b]chromone	(Nagatsu et al., 2002)
4	395.1834	395.1853	$C_{24}H_{27}O_5$	[M + H]$^+$	2,3-Dihydro-7-hydroxy-2R*,3R*-dimethyl-2-[4-methyl-5-(4-methyl-2- furyl)-3 (E),7-pentenyl]-furo[2,3-b]chromone	(Nagatsu et al., 2002)
5	383.2214	383.2217	$C_{24}H_{31}O_4$	[M + H]$^+$	2,3-dihydro-7-hydroxy-2S*, 3R*-dimethyl-3-[4,8-dimethyl-3(E),7-nonadienyl]-furo[3,2-c] coumarin	(Meng et al., 2013)
6	383.2214	383.2217	$C_{24}H_{31}O_4$	[M + H]$^+$	2,3-dihydro-7-hydroxy-2R*,3R*-dimethyl-3-[4,8-dimethyl-3(E),7-nona-dienyl]-furo[3,2-c]coumarin	(Meng et al., 2013)
7	383.2261	383.2217	$C_{24}H_{31}O_4$	[M + H]$^+$	2,3-dihydro-7-hydroxy-2S*,3R*-dimethyl-2-[4,8-dimethyl-3(E),7-nonadienyl]-furo[3,2-b]chromone	(Meng et al., 2013)
8	383.2219	383.2217	$C_{24}H_{31}O_4$	[M + H]$^+$	2,3-dihydro-7-hydroxy-2R*,3R*-dimethyl-2-[4,8-dimethyl-3(E),7-nonadienyl]-furo[3,2-b]chromone	(Meng et al., 2013)
9	383.2230	383.2217	$C_{24}H_{31}O_4$	[M + H]$^+$	Ferulin E	(Meng et al., 2013)
10	397.2389	397.2373	$C_{25}H_{33}O_4$	[M + H]$^+$	Ferulin D	(Meng et al., 2013)

preventing cancer cells from undergoing apoptosis (Zhang et al., 2020, Huang et al., 2021).

Western blot analysis was utilized to measure the expression levels of proteins associated with the mitochondrial apoptosis pathway and PI3K/Akt/Bad pathway. The results specifically showed that FF-EtOAc lowered the ratio of B-cell lymphoma-24(Bcl-2)/Bcl-2-associated X protein (Bax) and elevated the expression of cleaved Caspase-9, −3, and cleaved PARP in a dose-dependent way (Fig. 6A and 6B). The results also showed that FF-EtOAc concentration-dependently down-regulated the expression of p-Akt, p-GSK-3, and p-Bad, then elevated the expression of PTEN, but did not affect the protein levels of total Akt, GSK-3α/β, or Bad (Fig. 6C and 6D). All the results demonstrated that FF-EtOAc activated the mitochondrial and PI3K/Akt/Bad apoptotic pathways to cause apoptosis *in vitro.*

3.6. Effects of FF-EtOAc on growth inhibition in Eca-109 xenograft tumor nude mice and on apoptosis of Eca-109 cells in vivo

Female BALB/c nude mice were used to create Eca-109 subcutaneous tumor xenograft models, which were used to assess the therapeutic effectiveness of FF-EtOAc *in vivo*. When mice were treated with FF-EtOAc for 21 days, Eca-109 xenograft growth, volume, and weight were suppressed in dose-dependent way, but mice's weight did not significantly change (Fig. 7A and 7B).

Evaluation of the effect of FF-EtOAc on apoptosis production *in vivo* by TUNEL assay and IHC assay. TUNEL labeling of xenograft sections shows that the nuclei of apoptotic cells appear in fluorescent green and their number increases gradually in a dose-dependent manner (Fig. 7C). Meanwhile, the immunohistochemical assay results show that FF-EtOAc down-regulated the expression of p-Akt, but increased the expression of cleaved Caspase-3, (Fig. 7C). As per the results from HE staining, FF-EtOAc treatment caused chromatin agglutination and loosen the structure of tumor cells in a dose-dependent manner (Fig. 7C). Additionally, western blot analysis demonstrated that FF-EtOAc caused apoptosis *in vivo* activating the PI3K/Akt/Bad and mitochondrial apoptotic pathways, these results were shown by *in vitro* (Fig. 8A and 8B). Schematic summary of the mechanisms of FF-EtOAc induced EC cells apoptosis by mitochondrial and PI3K/Akt/Bad pathways in the present study (Fig. 9).

4. Discussion

Esophageal cancer was mainly occurred in the esophagus, and usually started in the cells inside the esophagus and can appeared anywhere in the esophagus. There are various treatments for esophageal cancer, such as surgery, radiotherapy, chemotherapy, etc., but they are criticized by cancer patients because of their poor healing process and side effects. Because natural products have low side effects, alleviate the symptoms of patients with cancer, prevent recurrence, and prolong survival, it was a hot area of anti-cancer research in the present today (Liu et al., 2019, Cao et al., 2021, Zhang et al., 2021).

The genus of *Ferula* L. was belonged to the family Umbelliferae, and it was a rare traditional Chinese medicine. There are more than 180 species of *Ferula* L. reported worldwide, and more than 20 species are mainly distributed in Xinjiang, and *Ferula ferulaeoides* (Steud.) Korovin was one of them. Additionally, the resin and roots of *F. ferulaeoides* have significant commercial and therapeutic potential in Xinjiang (Salehi et al., 2019, Liu et al., 2020). Although previous literature has acknowledged the anti-cancer potential of *F. ferulaeoides*, the specific anti-esophageal cancer mechanism remains underexplored (Li et al., 2018, Yao et al., 2020). In the meantime, our experiments demonstrate that FF-EtOAc had anti-proliferative effects on EC cells (Eca-109 and KYSE-150) and without significant toxicity to HEK293 cells. Moreover, FF-EtOAc could inhibit the migration activity of the EC cells as observed by cell migration assay and Transwell assay (Fig. 3 and Fig. 4).

Apoptosis, first described in 1972 as a form of programmed cell death (PCD) (Kerr et al., 1972, Kaczanowski 2016). It was utilized to get rid of undesirable cells in the early stages of growth. During adulthood, apoptosis is used to eliminate damaged cells and that prevents cancer from proliferating. It was could stop uncontrolled cell proliferation and tumor growth helps to prevent cancer (Riviere and Monteiro-Riviere 2010). Apoptotic cells generally showed cell shrinkage, while further shrunken cells break down into the apoptotic body. As stated by our study used Hoechst 33258 and Annexin V-FITC/PI double labeling, FF-EtOAc treatment triggered dose-dependent apoptosis in EC cells (Fig. 5.).

The membrane receptor pathway of apoptosis (extrinsic apoptotic pathway) and the biochemical mechanisms of cytochrome *C* released and Caspases activation (intrinsic apoptotic pathway)
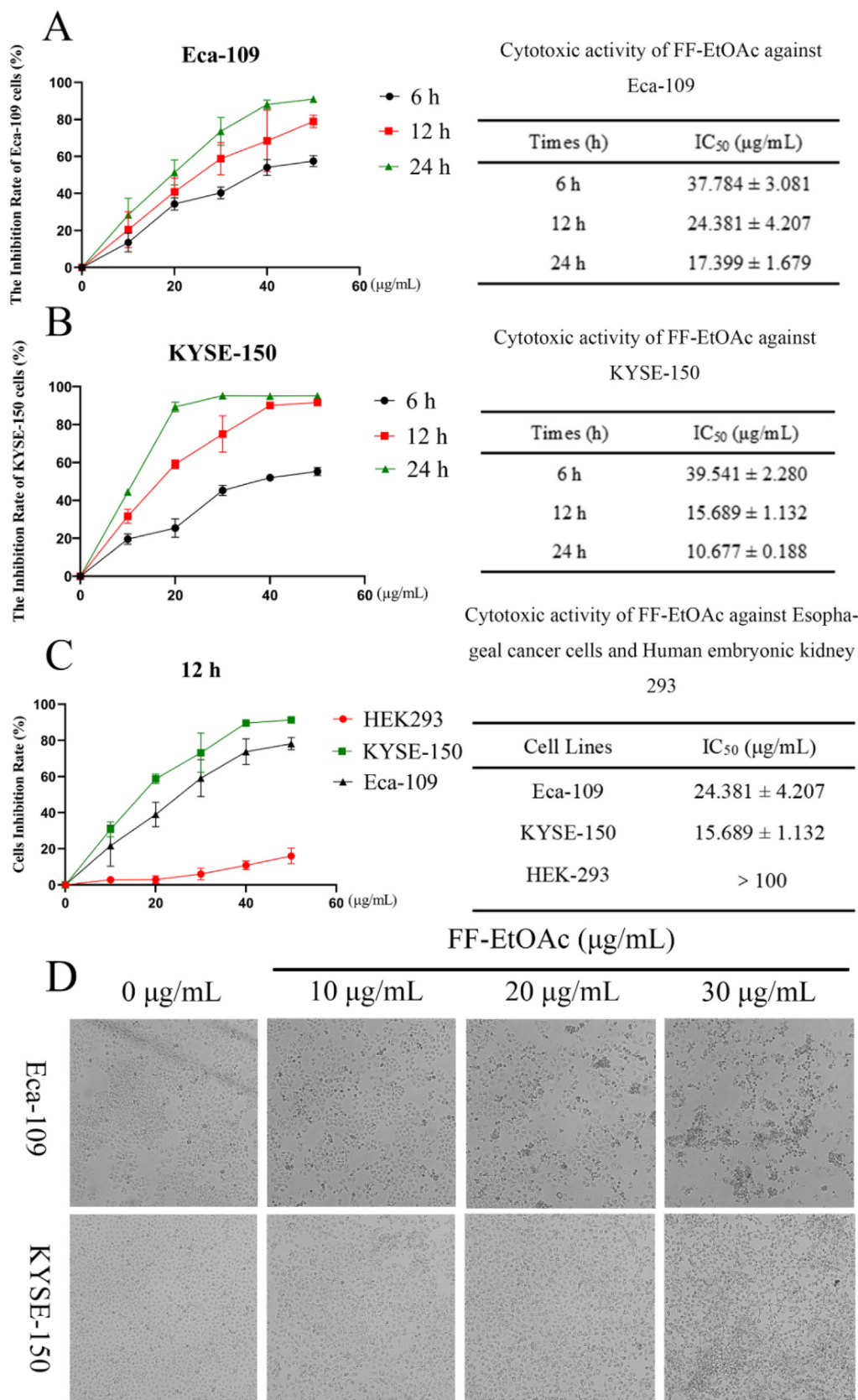
Fig. 3. FF-EtOAc inhibited the development of EC cells. (A and B) MTT assays were used to determine Eca-109 and KYSE-150 cells inhibition rates and IC$_{50}$ values after FF-EtOAc incubation for 6, 12, or 24 h (0, 10, 20, 30, 40, and 50 µg/mL). (C) MTT assays were used to determine Eca-109, KYSE-150 and HEK293 cells inhibition rates and IC$_{50}$ values after FF-EtOAc incubation 12 h (0, 10, 20, 30, 40, and 50 µg/mL). (D) The morphology of two EC cells after incubation with FF-EtOAc (0, 10, 20, and 30 µg/mL) for 12 h.
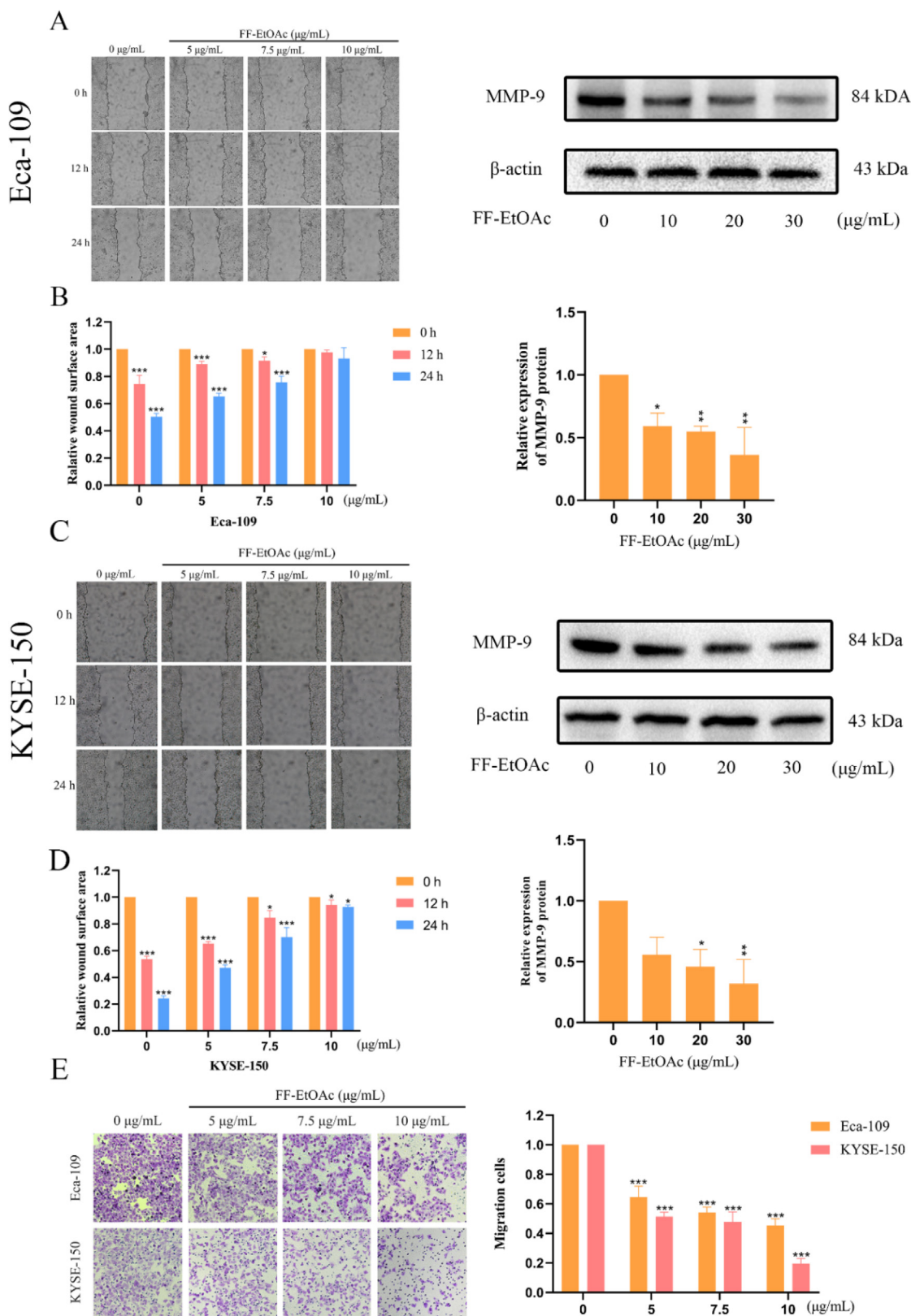
Fig. 4. Cell migration in EC cells is inhibited by FF-EtOAc. (A and B) In order to determine the effect of FF-EtOAc on the migration of Eca-109 cells, scratch wound healing experiments and Western blotting using β-actin as an internal control were employed to evaluate the expression levels of cell metastasis-related proteins. (C and D) In order to determine the effect of FF-EtOAc on the migration of KYSE-150 cells, scratch wound healing experiments and Western blotting using -actin as an internal control were employed to evaluate the expression levels of cell metastasis-related proteins. (E) In Transwell chambers treated with FF-EtOAc for 24 h, Eca-109 and KYSE150 cells were added, and the number of migrating cells was then counted. The control was β-actin. *$P < 0.05$, **$P < 0.01$ or ***$P < 0.001$ compare to control.
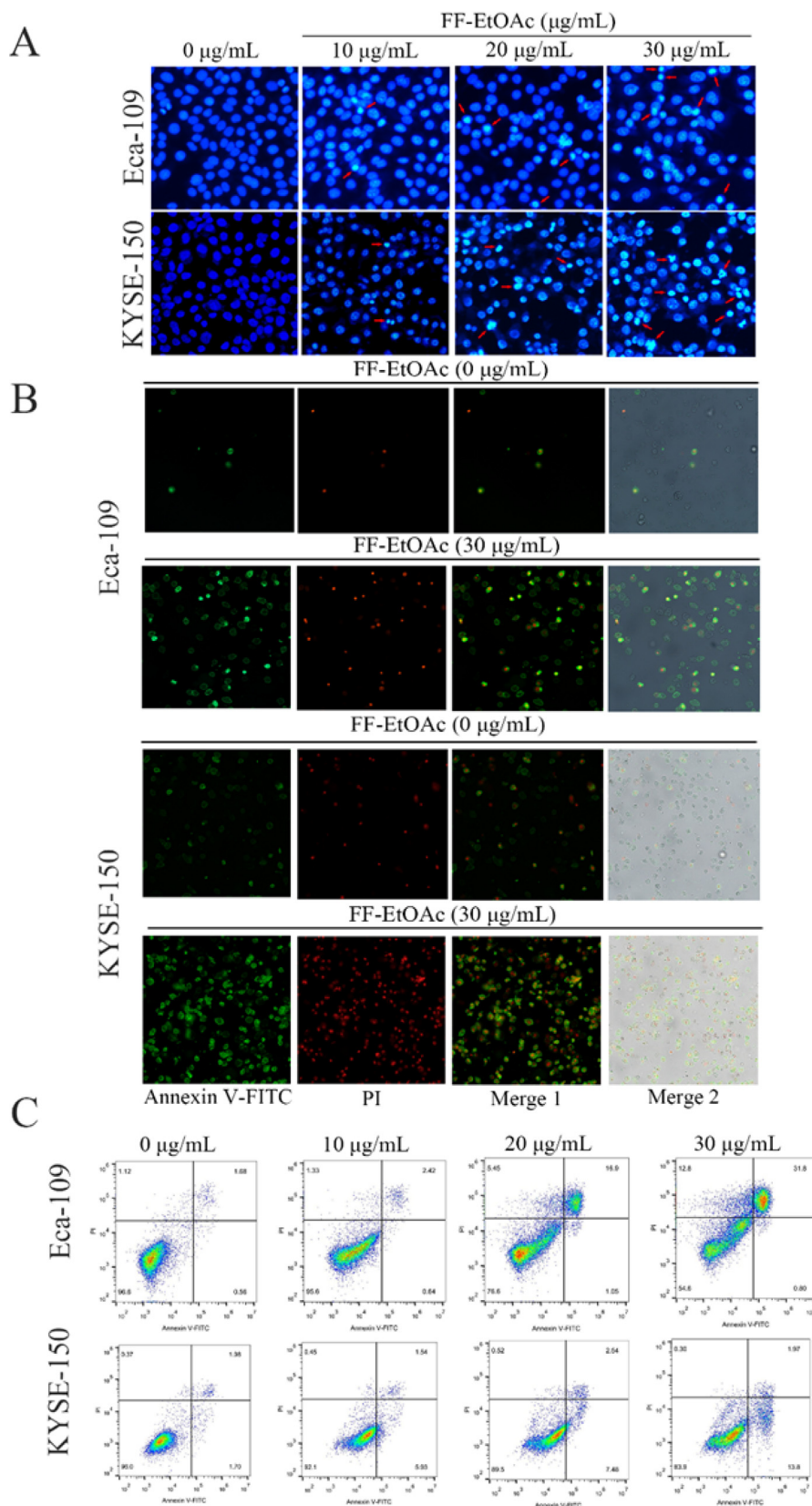
Fig. 5. FF-EtOAc induced apoptosis in EC cells. (A) Eca-109 cells and KYSE-150 cells were incubated with 0, 10, 20, and 30 µg/mL for 12 h and stained with Hoechst 33258. (B) Eca-109 cells and KYSE-150 cells were exposed to 0 and 30 µg/mL for 12 h before being stained with Annexin V/PI and examined under a fluorescence microscope. (C) Eca-109 cells and KYSE-150 cells were exposed to 0 and 30 µg/mL for 12 h. After Annexin V-FITC and PI labeling, the fraction of apoptosis was determined by flow cytometry.
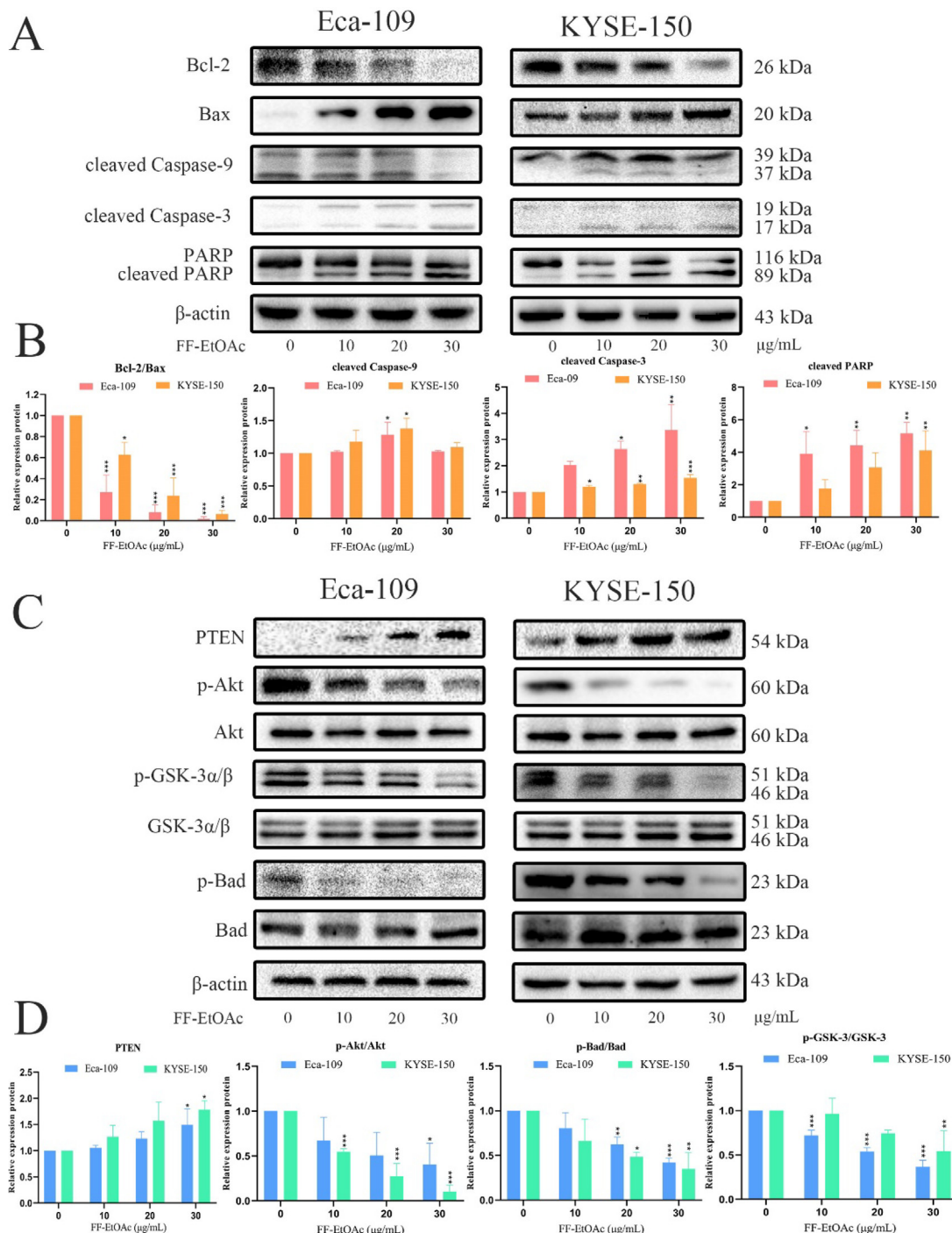
Fig. 6. *In vitro*, mitochondrial apoptotic and PI3K/Akt/Bad pathways were used by FF-EtOAc to induce apoptosis (A and B). By Western blot assay, the relative expression of Bcl-2/Bax, cleaved caspase-9 and caspase-3, and PARP was detected after FF-EtOAc treated laryngeal carcinoma cells (0, 10, 20, and 30 µg/mL) for 12 h. (C and D) Using Western blot assay, the relative expression of PTEN, p-Akt/Akt, p-Gsk-3/Gsk-3 and p-Bad/Bad was detected after FF-EtOAc treated laryngeal carcinoma cells (0, 10, 20, and 30 µg/mL) for 12 h. The control was β-actin. $*P < 0.05$, $**P < 0.01$ or $***P < 0.001$ compare to control.

were the primary pathways of the apoptosis mechanism (Cory and Adams 2002, Matthews et al., 2012). In the intrinsic apoptotic pathway, the Bcl-2 (B-cell leukemia/lymphoma-2) family is split into three parts, (1) anti-apoptotic protein (Bcl-2, Bcl-xl, BcldW, Mcl-1, and BFL-1/A1), (2) pro-apoptotic protein (Bax, Bak, and Bok) and (3) pro-apoptotic BH_3-only protein (Bad, Bid, Bik, Bim, BMF, HRK, Noxa, and PUMA). First, the anti-apoptotic (Bcl-2) was inhibited, and the pro-apoptotic (Bax) was activated. As a result, cytochrome *C* diffuses into the cytoplasm and mitochondrial outer

membrane permeability (MOMP) is altered. Cytochrome *C* binded to Apaf-1, and resulted in pro-Caspase-9 and pro-Caspase-3 proteolytic activation in the cytoplasm, cleaving the cell substrate and inducing apoptosis (Kashyap et al., 2021). According to the study, treatment with FF-EtOAc can enhance the expression of pro-Caspase-9, pro-Caspase-3, and Bax, and decreased the expression of Bcl-2 both *in vitro* and *in vivo* (Fig. 6 A, Fig. 6 B, and Fig. 8 A).

The phosphoinositide3-kinase (PI3K) is a member of the proto-oncogene family, it's an important kinase for inositol and phos-
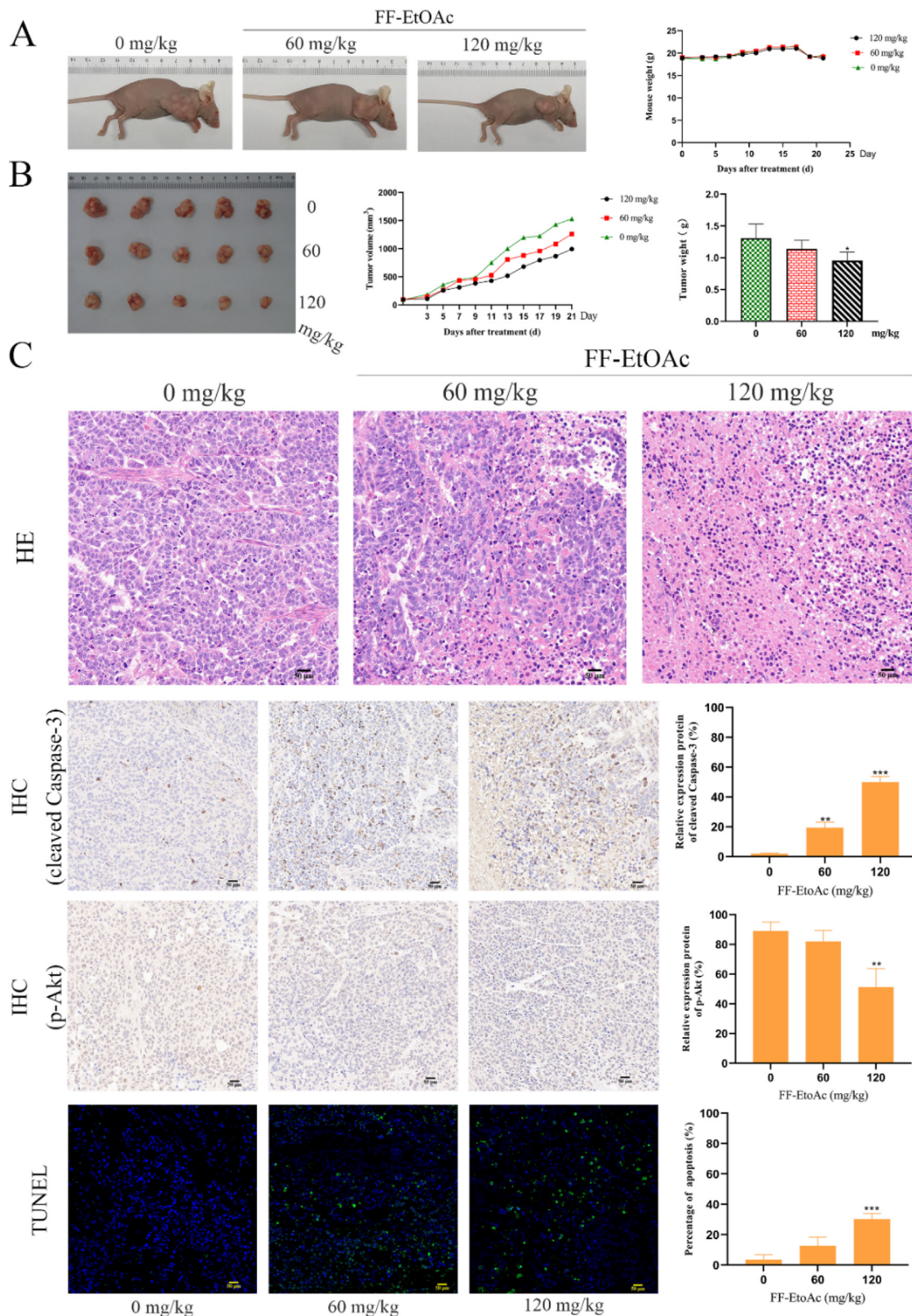
Fig. 7. Apoptosis and the inhibitory effect *in vivo* of FF-EtOAc on transplanted tumors. (A and B) After treated with FF-EtOAc (0, 60 and 120 mg/kg) for 21 days, then We dissected tumors from the control and FF-EtOAc-treated mice. The tumor volume, tumor weight, and mouse weight were also counted. (C) Prepared tumor slices underwent TUNEL analysis. The green fluorescence stains in the Tunel experiment showed that the FF-EtOAc-treated mice's tumors underwent apoptosis. Eca-109 inoculated mouse tumor tissue samples were produced and IHC-tested. Manifestations of cleaved Caspase-3 and p-Akt were pictured and quantified by IHC. $*P < 0.05$, $**P < 0.01$ or $***P < 0.001$ compare to control.
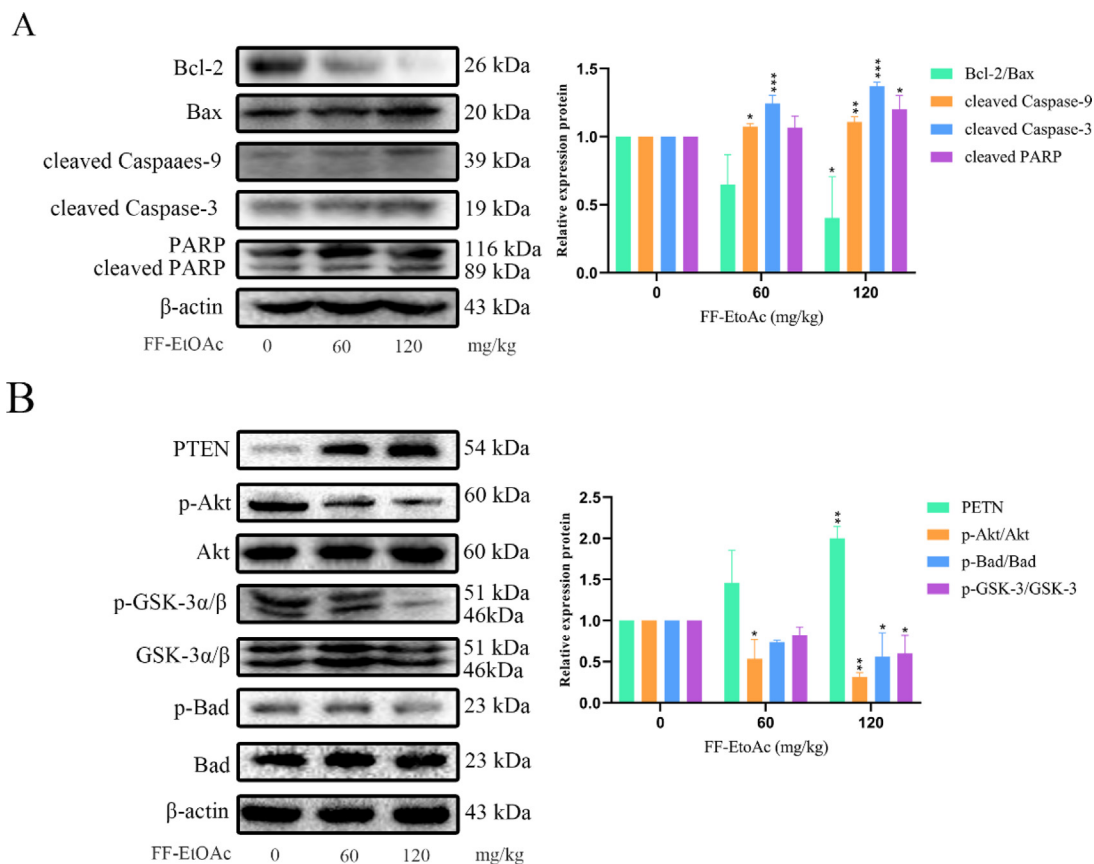
Fig. 8. *In vivo*, FF-EtOAc caused apoptosis via the PI3K/Akt/Bad and mitochondrial apoptotic pathway. (A) By using Western blot technique, it was possible to identify the relative expression of Bcl-2/Bax, cleaved caspase-9 and caspase-3, and PARP in malignancies. (B) By Western blot assay, the relative expression of PTEN, p-Akt/Akt, p-Gsk-3/Gsk-3, and p-Bad/Bad was detected from tumors. The control was β-actin. $*P < 0.05$, $**P < 0.01$ or $***P < 0.001$ compare to control.
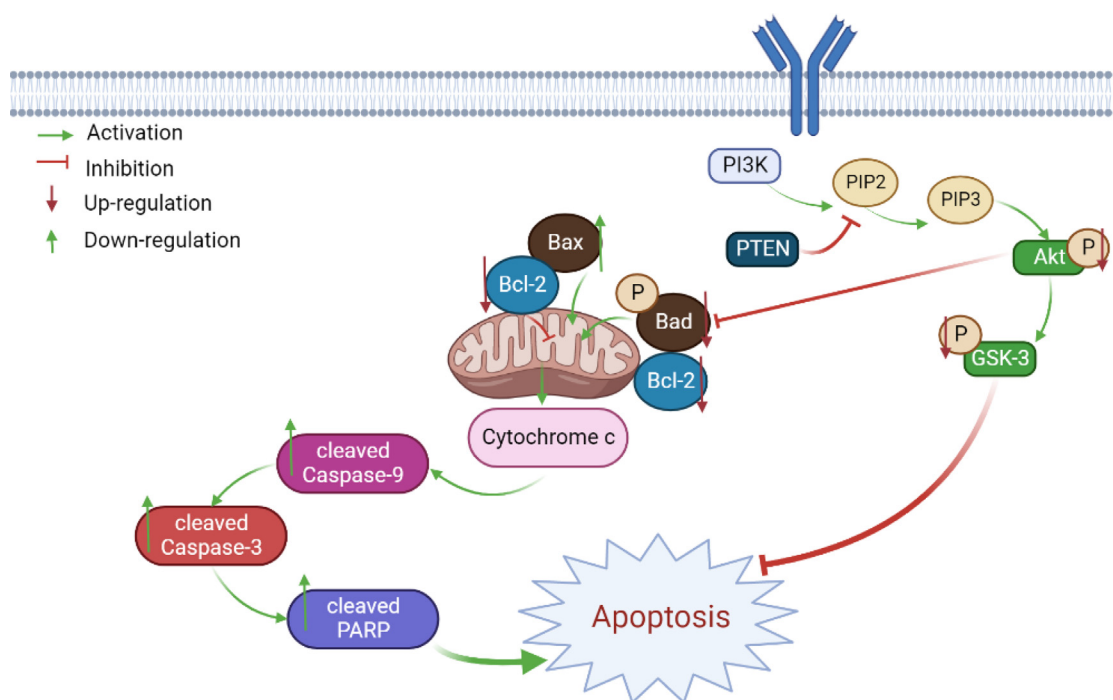
Fig. 9. Schematic summary of the mechanisms of FF-EtOAc induced EC cell apoptosis in the present study.

phatidylinositol. Under normal conditions, lipid-like products are produced by their activation. The lipid products produced by its activation are three types, and phosphatidylinositol 3,4,5-triphosphate [PI (3,4,5) P3] is one of them. It was also called Akt (also known as protein kinase B, PKB), it was a serine/threonine protein kinase with a molecular weight of approximately 60 kDa. Akt could be divided into three isoforms (AKT1, AKT2, AKT3 or PKBα, PKBβ, PKBγ), which have different but all have overlapping functions. (Osaki et al., 2004). As a downstream protein of PI3K, Akt had two major phosphorylation sites, Thr308 and Ser473. PI3K could not directly activate Akt, but it's by binded to the intracellular PH domain-containing signaling protein Akt and phosphoinositide-dependent kinase I (PDK1), which induced Akt to the cell membrane and then catalyzes the phosphorylation of the Thr308 site of the Akt protein, thus partially activating Akt, but phosphorylation of Ser473 is required for the full functional activity of Akt. It was found that inactivation of PTEN loss leads to activation of the PI3K/Akt pathway and that EGFR overexpression or mutation also produces these types of results. (Colakoglu et al., 2008, Alvarez-Garcia et al., 2019, Aboelez et al., 2023).

Glycogen synthesis kinase 3 (GSK-3), a serine/threonine kinase, had been found to have two isoforms, GSK3α and GSK3β. GSK3β acted as a substrate in the PI3K/Akt pathway, a downstream protein that interacts directly with Akt and is involved in the cell proliferation process (Woodgett 1990, Cross et al., 1995). Bad is a member of the Bcl-2 family of pro-apoptotic BH$_3$-only protein (Xu et al., 2021).

Through phosphorylation of serine 473 (Ser473), PI3K activates Akt's function. Activated Akt can then deactivate pro-apoptotic proteins (Bad) and activate proteins that prevent apoptosis through the process of phosphorylation (Bak et al., 2011, Benvenuto et al., 2017). After being phosphorylated by Akt, GSK3 is inactivated, which consequently prevented the onset of apoptosis (Eléonore Beurel and Richard S Jope 2006). *in vitro* and *vivo*, FF-EtOAc caused apoptosis in EC cells via the PI3K/Akt/Bad signaling pathway, according to a Western blot study of the relevant protein expression (Fig. 6C and 6D; Fig. 8B). In a nutshell, our work showed that FF-EtOAc significantly reduced the proliferation and migration of EC cells (Eca-190 and KYSE-150) and had lower toxicity to HEK293 cells. After *in vivo* and *in vitro* experiments, it was determined that FF-EtOAc could induce apoptosis in EC cells, and further verified that FF-EtOAc triggers apoptosis in EC cells under PI3K/Akt/Bad pathway and mitochondrial apoptosis pathway. This also suggests that FF-EtOAc could be investigated further as a potential drug for the treatment of esophageal cancer.

5. Conclusion

In conclusion, FF-EtOAc can effectively inhibit EC cell growth and enhance apoptosis partly by inhibiting the PI3K/Akt/Bad and mitochondrial pathway *in vivo* and *in vitro*. These findings provide strong evidence for the potential of FF-EtOAc as a chemotherapeutic drug for esophageal carcinoma.

6. Ethics statements

The "Guidelines for Tumor Induction in Mice and Rats, Animal Care and Use Committee of South-Central Minzu University " were followed in the conduct of this work. The "Animal Care and Use Committee of South-Central Minzu University" gave its approval to the procedure. The final manuscript draft has been approved by all writers, who also agree to be responsible for the entire piece of work.

7. Institutional review board statement

The "Guidelines for Tumor Induction in Mice and Rats, Animal Care and Use Committee of South-Central Minzu University" were followed in the conduct of this work. The "Animal Care and Use Committee of South-Central Minzu University" gave its approval to the procedure. The final manuscript draft has been approved by all writers, who also agree to be responsible for the entire piece of work.

CRediT authorship contribution statement

Yerlan Bahetjan: Writing – original draft, Visualization, Investigation, Formal analysis, Data curation. **Wenqi Liu:** Data curation. **Muguli Muhaxi:** Resources. **Ni Zheng:** Data curation. **Fatemeh Sefidkon:** Resources. **Kejian Pang:** Resources. **Guangwen Shu:** Supervision, Writing – review & editing, Project administration, Conceptualization. **Xinzhou Yang:** Supervision, Writing – review & editing, Project administration, Funding acquisition, Conceptualization.

Declaration of Competing Interest

The authors declare that they have no known competing financial interests or personal relationships that could have appeared to influence the work reported in this paper.

References

Aboelez, M.O., Kamel, M.S., Belal, A., et al., 2023. Microwave-assisted synthesis, spectroscopic characterization, and biological evaluation of fused thieno[2,3-d] pyrimidines as potential anti-cancer agents targeting EGFR(WT) and EGFR (T790M). Mol. Divers. 27, 901–917. https://doi.org/10.1007/s11030-022-10477-7.

Ahmed, S.A., Kamel, M.S.M., Aboelez, O., et al., 2022. Thieno[2,3-b]thiophene derivatives as potential EGFR(WT) and EGFRT(790M) inhibitors with antioxidant activities: Microwave-assisted synthesis and quantitative in vitro and in silico studies. ACS Omega 7, 45535–45544. https://doi.org/10.1021/acsomega.2c06219.

Alvarez-Garcia, V., Tawil, Y., Wise, H.M., et al., 2019. Mechanisms of PTEN loss in cancer: It's all about diversity. Semin. Cancer Biol. 59, 66–79. https://doi.org/10.1016/j.semcancer.2019.02.001.

Asemani, Y., Azadmehr, A., Hajiaghaee, R., et al., 2018. Anticancer potential of Ferula hezarlalehzarica Y. Ajani fraction in Raji lymphoma cell line: induction of apoptosis, cell cycle arrest, and changes in mitochondrial membrane potential. Daru 26, 143–154. https://doi.org/10.1007/s40199-018-0219-z.

Atanasov, A. G., Zotchev, S. B., V. Dirsch, M., et al., 2021. Natural products in drug discovery: advances and opportunities. Nat Rev Drug Discov. 20, 200-216. https://doi.org/10.1038/s41573-020-00114-z.

Bak, Y., Kim, H., Kang, J.W., et al., 2011. A synthetic naringenin derivative, 5-hydroxy-7,4'-diacetyloxyflavanone-N-phenyl hydrazone (N101–43), induces apoptosis through up-regulation of Fas/FasL expression and inhibition of PI3K/Akt signaling pathways in non-small-cell lung cancer cells. J. Agric. Food Chem. 59, 10286–10297. https://doi.org/10.1021/jf2017594.

Bashir, S., Alam, M., Adhikari, A., et al., 2014. New antileishmanial sesquiterpene coumarins from Ferula narthex Boiss. Phytochem. Lett. 9, 46–50. https://doi.org/10.1016/j.phytol.2014.04.009.

Benvenuto, M., Mattera, R., Masuelli, L., et al., 2017. (+/-)-Gossypol induces apoptosis and autophagy in head and neck carcinoma cell lines and inhibits the growth of transplanted salivary gland cancer cells in BALB/c mice. Int. J. Food Sci. Nutr. 68, 298–312. https://doi.org/10.1080/09637486.2016.1236077.

Bray, F., Ferlay, J., Soerjomataram, I., et al., 2018. Global cancer statistics 2018: GLOBOCAN estimates of incidence and mortality worldwide for 36 cancers in 185 countries. CA Cancer J. Clin. 68, 394–424 https://www.ncbi.nlm.nih.gov/pubmed/30207593.

Cao, L., Wang, X., Zhu, G., et al., 2021. Traditional Chinese medicine therapy for esophageal cancer: A literature review. Integr. Cancer Ther. 20. https://doi.org/10.1177/15347354211061720.

Chen, H., Yuan, J., Hao, J., et al., 2019. alpha-Humulene inhibits hepatocellular carcinoma cell proliferation and induces apoptosis through the inhibition of Akt signaling. Food Chem. Toxicol. 134,. https://doi.org/10.1016/j.fct.2019.110830 110830.

Chinese Pharmacopoeia Commission, 2020. Pharmacopoeia of People's Republic of China. Beijing, China Medical Science Press.

Colakoglu, T., Yildirim, S., Kayaselcuk, F., et al., 2008. Clinicopathological significance of PTEN loss and the phosphoinositide 3-kinase/Akt pathway in sporadic colorectal neoplasms: is PTEN loss predictor of local recurrence? Am. J. Surg. 195, 719–725. https://doi.org/10.1016/j.amjsurg.2007.05.061.

Cory, S., Adams, J.M., 2002. The Bcl2 family: regulators of the cellular life-or-death switch. Nat. Rev. Cancer 2, 647–656. https://doi.org/10.1038/nrc883.

Cross, D.A., Alessi, D.R., Cohen, P., et al., 1995. Inhibition of glycogen synthase kinase-3 by insulin mediated by protein kinase B. Nature 378, 785–789. https://doi.org/10.1038/378785a0.

Charlene, DeHaven., 2014. Chemotherapy and radiotherapy effects on the skin. Plast Surg Nurs. 34, 192-195. https://doi.org/10.1097/PSN.0000000000000077.

Eléonore, B., Richard, S.J., 2006. The paradoxical pro- and anti-apoptotic actions of GSK3 in the intrinsic and extrinsic apoptosis. Prog. Neurobiol. 79, 173–189. https://doi.org/10.1016/j.pneurobio.2006.07.006.

He, F., Wang, J., Liu, L., et al., 2021. Esophageal cancer: trends in incidence and mortality in China from 2005 to 2015. Cancer Med. 10, 1839–1847. https://doi.org/10.1002/cam4.3647.

He, J.K., Wu, X.S., Wang, Y., et al., 2013. Growth inhibitory effects and molecular mechanisms of crotoxin treatment in esophageal Eca-109 cells and transplanted tumors in nude mice. Acta Pharmacol. Sin. 34, 295–300. https://doi.org/10.1038/aps.2012.156.

Homs, M.Y.V., Voest, E.E., Siersema, P.D., 2009. Emerging drugs for esophageal cancer. Expert Opin. Emerg. Drugs 14, 329–339. https://doi.org/10.1517/14728210902976842.

Howell, S., Shalet, S., 1998. Gonadal damage from chemotherapy and radiotherapy. Endocrinol. Metab. Clin. North Am. 27, 927–943. https://doi.org/10.1016/s0889-8529(05)70048-7.

Huang, H., Hao, J., Pang, K., et al., 2020. A biflavonoid-rich extract from Selaginella moellendorffii Hieron. induces apoptosis via STAT3 and Akt/NF-kappaB signalling pathways in laryngeal carcinoma. J. Cell Mol. Med. 24, 11922–11935. https://doi.org/10.1111/jcmm.15812.

Huang, H., Peng, Y., Zhou, T., et al., 2021. A composition of bractatin and neobractatin from the fruits of Garciniabracteatainduces apoptosis in throat cancer through the endoplasmic reticulum stress, mitochondrial apoptotic and Akt pathways. J. Funct. Foods 84,. https://doi.org/10.1016/j.jff.2021.104585 104585.

Isaka, K., Nagatsu, A., Ondognii, P., et al., 2001. Sesquiterpenoid derivatives from Ferula ferulaeoides [correction of ferulioides]. V. Chem. Pharm. Bull. (Tokyo) 49, 1072–1076. https://doi.org/10.1248/cpb.49.1072.

Kaczanowski, S., 2016. Apoptosis: its origin, history, maintenance and the medical implications for cancer and aging. Phys. Biol. 13,. https://doi.org/10.1088/1478-3975/13/3/031001 031001.

Kakeji, Y., Oshikiri, T., Takiguchi, G., et al., 2021. Multimodality approaches to control esophageal cancer: development of chemoradiotherapy, chemotherapy, and immunotherapy. Esophagus 18, 25–32. https://doi.org/10.1007/s10388-020-00782-1.

Kashyap, D., Garg, V.K., Goel, N., et al., 2021. Intrinsic and extrinsic pathways of apoptosis: Role in cancer development and prognosis. Adv. Protein Chem. Struct. Biol. 125, 73–120. https://doi.org/10.1016/bs.apcsb.2021.01.003.

Kato, H., Nakajima, M., 2013. Treatments for esophageal cancer: a review. Gen. Thorac. Cardiovasc. Surg. 61, 330–335. https://doi.org/10.1007/s11748-013-0246-0.

Kerr, J.F., Wyllie, A.H., Currie, A.R., et al., 1972. Apoptosis: a basic biological phenomenon with wide-ranging implications in tissue kinetics. Br. J. Cancer 26, 239–257. https://doi.org/10.1038/bjc.1972.33.

Kim, K.H., Lee, H.J., Jeong, S.J., et al., 2011. Galbanic acid isolated from Ferula assafoetida exerts in vivo anti-tumor activity in association with anti-angiogenesis and anti-proliferation. Pharm. Res. 28, 597–609. https://doi.org/10.1007/s11095-010-0311-7.

Li, X.X., Zhang, S.J., Chiu, A.P., et al., 2018. Targeting of AKT/ERK/CTNNB1 by DAW22 as a potential therapeutic compound for malignant peripheral nerve sheath tumor. Cancer Med. 7, 4791–4800. https://doi.org/10.1002/cam4.1732.

Liu, T., Wang, L., Zhang, L., et al., 2020. Insecticidal, cytotoxic and anti-phytopathogenic fungal activities of chemical constituents from the aerial parts of Ferula sinkiangensis. Nat. Prod. Res. 34, 1430–1436. https://doi.org/10.1080/14786419.2018.1509328.

Liu, C., Yang, S., Wang, K., et al., 2019. Alkaloids from Traditional Chinese Medicine against hepatocellular carcinoma. Biomed. Pharmacother. 120,. https://doi.org/10.1016/j.biopha.2019.109543 109543.

Liu, M.M., Zhang, S.W., Liu, Q.G., et al., 2020. Microscopic anatomy and ultrastructure of the resin ducts of Ferula ferulaeoides (Steud.) Korov. in Xinjiang. Microsc. Res. Tech. 83, 1566–1573. https://doi.org/10.1002/jemt.23552.

Mahendra, P., Bisht, S., 2012. Ferula asafoetida: Traditional uses and pharmacological activity. Pharmacogn. Rev. 6, 141–146. https://doi.org/10.4103/0973-7847.99948.

Matthews, G., Newbold, M., Johnstone, A.R.W., et al., 2012. Intrinsic and extrinsic apoptotic pathway signaling as determinants of histone deacetylase inhibitor antitumor activity. Adv. Cancer Res. 116, 165–197. https://doi.org/10.1016/B978-0-12-394387-3.00005-7.

Meng, H., Li, G., Huang, J., et al., 2013. Sesquiterpene coumarin and sesquiterpene chromone derivatives from Ferula ferulaeoides (Steud.) Korov. Fitoterapia 86, 70–77. https://doi.org/10.1016/j.fitote.2013.02.002.

Nagatsu, A., Isaka, K., Kojima, K., et al., 2002. New sesquiterpenes from Ferula ferulaeoides (Steud.) Korovin. VI. Isolation and identification of three new dihydrofuro[2,3-b]chromones. Chem. Pharm. Bull. (Tokyo) 50, 675–677. https://doi.org/10.1248/cpb.50.675.

Osaki, M., Oshimura, M., Ito, H., et al., 2004. PI3K-Akt pathway: its functions and alterations in human cancer. Apoptosis 9, 667–676. https://doi.org/10.1023/B:APPT.0000045801.15585.dd.

Rahali, F.Z., Kefi, S., Bettaieb, R.I., et al., 2018. Phytochemical composition and antioxidant activities of different aerial parts extracts of Ferula communis L. Plant Biosyst. - Int. J. Dealing Asp. Plant Biol. 153, 213–221. https://doi.org/10.1080/11263504.2018.1461696.

Riviere, J. E., Monteiro-Riviere, N. A., 2010. Dermal Exposure and Absorption of Chemicals and Nanomaterials. Reference Module in Biomedical Sciences. McQueen and Charlene A. London, Elsevier. 1: 111-122.

Salehi, M., Naghavi, M.R. Bahmankar, M., 2019. A review of Ferula species: Biochemical characteristics, pharmaceutical and industrial applications, and suggestions for biotechnologists. Ind. Crop. Prod. 139,. https://doi.org/10.1016/j.indcrop.2019.111511 111511.

Sattar, Z., Iranshahi, M., 2017. Phytochemistry and pharmacology of Ferula persica Boiss.: A review. Iran. J. Basic Med. Sci. 20, 1–8. https://doi.org/10.22038/ijbms.2017.8085.

Shay, G., Lynch, C.C., Fingleton, B., 2015. Moving targets: Emerging roles for MMPs in cancer progression and metastasis. Matrix Biol. 44–46, 200–206. https://doi.org/10.1016/j.matbio.2015.01.019.

Sonigra, P., Meena, M., 2020. Metabolic profile, bioactivities, and variations in the chemical constituents of essential oils of the Ferula Genus (Apiaceae). Front. Pharmacol. 11,. https://doi.org/10.3389/fphar.2020.608649 608649.

Sung, H., Ferlay, J., Siegel, R.L., et al., 2021. Global cancer statistics 2020: GLOBOCAN estimates of incidence and mortality worldwide for 36 cancers in 185 countries. CA Cancer J. Clin. 71, 209–249. https://doi.org/10.3322/caac.21660.

Tavassoli, M., Jalilzadeh-Amin, G., Fard, V.R.B., et al., 2018. The in vitro effect of Ferula asafoetida and Allium sativum extracts on Strongylus spp. Ann. Parasitol. 64, 59–63. https://doi.org/10.17420/ap6401.133.

Utegenova, G.A., Pallister, K.B., Kushnarenko, S.V., et al., 2018. Chemical composition and antibacterial activity of essential oils from Ferula L. species against methicillin-resistant Staphylococcus aureus. Molecules 23, 1679. https://doi.org/10.3390/molecules23071679.

Watanabe, M., Otake, R., Kozuki, R., et al., 2020. Recent progress in multidisciplinary treatment for patients with esophageal cancer. Surg. Today 50, 12–20. https://doi.org/10.1007/s00595-019-01878-7.

Woodgett, J.R., 1990. Molecular cloning and expression of glycogen synthase kinase-3/factor A. EMBO J. 9, 2431–2438. https://doi.org/10.1002/j.1460-2075.1990.tb07419.x.

Xu, Y.X., Jiang, Y.P., Wang, Y.Z., et al., 2021. LINC00473 rescues human bone marrow mesenchymal stem cells from apoptosis induced by dexamethasone through the PEBP1-mediated Akt/Bad/Bcl-2 signaling pathway. Int. J. Mol. Med. 41, 171–182. https://doi.org/10.3892/ijmm.2020.4788.

Yao, D., Pan, D., Zhen, Y., et al., 2020. Ferulin C triggers potent PAK1 and p21-mediated anti-tumor effects in breast cancer by inhibiting Tubulin polymerization in vitro and in vivo. Pharmacol. Res. 152,. https://doi.org/10.1016/j.phrs.2019.104605 104605.

Yarizade, A., Hasani, K.H., Niazi, A., 2017. In vitro antidiabetic effects of ferula Assa-Foetida extracts through dipeptidyl peptidase Iv and α-glucosidase inhibitory activity. Asian J. Pharm. Clin. Res. 10, 357. https://doi.org/10.22159/ajpcr.2017.v10i5.16648.

Zhang, R., Hao, J., Wu, Q., et al., 2020. Dehydrocostus lactone inhibits cell proliferation and induces apoptosis by PI3K/Akt/Bad and ERS signalling pathway in human laryngeal carcinoma. J. Cell Mol. Med. 24, 6028–6042. https://doi.org/10.1111/jcmm.15131.

Zhang, X., Qiu, H., Li, C., et al., 2021. The positive role of traditional Chinese medicine as an adjunctive therapy for cancer. Biosci. Trends 15, 283–298. https://doi.org/10.5582/bst.2021.01318.

Zhang, L., Tong, X., Zhang, J., et al., 2015. DAW22, a natural sesquiterpene coumarin isolated from Ferula ferulaeoides (Steud.) Korov. that induces C6 glioma cell apoptosis and endoplasmic reticulum (ER) stress. Fitoterapia 103, 46–54. https://doi.org/10.1016/j.fitote.2015.03.010.

Znati, M., Hichem, B.J., Cazaux, S., et al., 2014. Chemical composition, biological and cytotoxic activities of plant extracts and compounds isolated from Ferula lutea. Molecules 19, 2733–2747. https://doi.org/10.3390/molecules19032733.